The inflammatory chemokine Cxcl18b exerts neutrophil-specific chemotaxis via the promiscuous chemokine receptor Cxcr2 in zebrafish

Vincenzo Torraca, Natasja A. Otto, Aidin Tavakoli-Tameh and Annemarie H. Meijer*

Affiliation

Institute of Biology, Leiden University, The Netherlands

* Corresponding author

prof. dr. Annemarie H. Meijer

e-mail: a.h.meijer@biology.leidenuniv.nl

address: Institute of Biology, Leiden University, Einsteinweg 55, 2333 CC, Leiden, The Netherlands

Highlights

- The zebrafish chemokine Cxcl18b is chemotactic towards neutrophils
- Cxcl18b requires expression of Cxcr2 to elicit neutrophil recruitment
- During infection, Cxcl18b is induced in cells neighbouring the infectious focus
- Cxcl18b is expressed by uninfected stromal cells within *M. marinum* granulomas

Abstract

Cxcl18b is a chemokine found in zebrafish and in other piscine and amphibian species. Cxcl18b is a reliable inflammatory marker; however, its function is yet to be elucidated. Here, we found that Cxcl18b is chemotactic towards neutrophils, similarly to Cxcl8a/Interleukin-8, the best characterised neutrophil chemoattractant in humans and

teleosts. Like Cxcl8a, Cxcl18b-dependent recruitment required the chemokine receptor Cxcr2, while it was unaffected by depletion of the other two neutrophil receptors *cxcr1* and *cxcr4b.* To visualise *cxcl18b* induction, we generated a *Tg(cxcl18b:eGFP)* reporter line. The transgene is induced locally upon bacterial infection with the fish pathogen *Mycobacterium marinum*, but strikingly is not directly expressed by infected cells. Instead, *cxcl18b* is induced by non-phagocytic uninfected cells that compose the stroma of the granulomas, typical inflammatory lesions formed upon mycobacterial infections. Together, these results suggest that Cxcl18b might be an important contributor to neutrophil chemotaxis in the inflammatory microenvironment and indicate that the zebrafish model could be explored to further investigate *in vivo* the biological relevance of different Cxcl8-like chemokine lineages.

Keywords

Neutrophil chemotaxis; *Mycobacterium marinum*; Inflammatory chemokine; Zebrafish; Innate immunity; Leukocyte biology.

1. Introduction

Chemokines are a family of small cell-signalling proteins that direct the migration of cells expressing the corresponding receptors across a ligand concentration gradient. These potent chemotactic molecules play complex pleiotropic functions in the control of the immune response and of host-pathogen interactions (Zlotnik and Yoshie, 2012). The zebrafish (*Danio rerio*) is an attractive vertebrate model to study this complexity *in vivo*, as it provides both a genetically tractable system, to generate new genetically-encoded tools, and an optically-accessible platform to follow the dynamics of immune cells and processes intravitally (Harvie and Huttenlocher, 2015; Torraca et al., 2014). The transparency of the zebrafish allows direct visualisation of cellular migration processes in response to chemotactic cues and infections. To facilitate *in vivo* analysis, many fluorescent reporter lines have been developed that label different immune cell types, including macrophages and neutrophils (Ellett et al., 2011; Mathias et al., 2009; Renshaw et al., 2006). Additionally, the use of the zebrafish has been extended by combining the optical properties of this model with pharmacological and genetic tools that well apply to this species, due to high permeability

to compounds by submersion and to the ease of application of gene editing techniques (de Oliveira et al., 2013; Hruscha and Schmid, 2015).

A CXC subgroup of chemokines (containing the Cysteine-X-Cysteine motif) exists in both mammalian and teleost species. In mammals, this family can be further divided into ELR+ and ELR− chemokines, based on the presence or absence of the Glutamic acid-Leucine-Arginine motif preceding the CXC sequence. ELR+ chemokines include CXCL1-2-3 (GRO-α-β-γ, Growth-regulated protein alpha, beta, gamma), CXCL5 (ENA-78, Epithelial-derived neutrophil-activating peptide 78), CXCL6 (GCP-2, Granulocyte chemotactic protein 2), CXCL7 (NAP-2, Neutrophil-activating peptide 2) and CXCL8 (IL-8, Interleukin-8). These are potent chemoattractants of neutrophils (Ahuja and Murphy, 1996; Clark-Lewis et al., 1993; Pelus et al., 2002; Russo et al., 2014; Van Damme et al., 1989; Wolf et al., 1998), while ELR− chemokines, such as CXCL9 (MIG, Monokine induced by gamma interferon), CXCL10 (IP-10, Interferon gamma-inducible protein 10) and CXCL11 (I-TAC, Interferon-inducible T-cell alpha chemoattractant), are best known for the attraction of lymphocytes and monocyte/macrophages and possess poor chemotactic ability towards neutrophils. In fish, the ELR sequence is not conserved in chemokines that exert neutrophil chemotactic properties (Cai et al., 2009). However, it has been demonstrated that the zebrafish Cxcl8/Il-8 paralogues, despite being ELR-deficient, are still potent attractors of neutrophils (de Oliveira et al., 2013; Deng et al., 2013; Sarris et al., 2012).

CXCL8 is the best-studied neutrophil chemoattractant in humans (Russo et al., 2014; Van Damme et al., 1989) and is conserved in zebrafish (de Oliveira et al., 2013; Deng et al., 2013; Sarris et al., 2012), while absent in rodents (Mukaida, 2003; Tanino et al., 2010). In both zebrafish and mammals, Cxcl8/CXCL8 signals via the receptor Cxcr2/CXCR2 (de Oliveira et al., 2013; Deng et al., 2013; Russo et al., 2014). In mice this receptor still exerts a chemotactic activity towards neutrophils, but this is evoked by binding to other ELR+ chemokines (CXCL1-2-3-5-7) (Russo et al., 2014), to the non-chemokine tripeptide PGP (Pro-Gly-Pro, a molecule that derives from extracellular matrix breakdown) (Weathington et al., 2006), and to MIF (Macrophage migration

inhibitory factor, a non-chemokine component which inhibits macrophage migration but sustains neutrophil recruitment) (Bernhagen et al., 2007). The CXCR2 receptor is promiscuous in humans too and can respond to CXCL1-2-3-5-6-7-8 (Ahuja and Murphy, 1996; Russo et al., 2014; Wolf et al., 1998), PGP (Gaggar et al., 2008; Weathington et al., 2006) and MIF (Bernhagen et al., 2007). Finally, in humans, the activity of CXCL8 is non-specific for CXCR2, since this ligand, together with CXCL6, can also induce neutrophil chemotaxis via CXCR1, another chemokine receptor, closely related to CXCR2 (Stillie et al., 2009). We currently know that two zebrafish Cxcl8 chemokines, Cxcl8a (ENSDARG00000104795, also known as Cxcl8-l1 or Il8) and Cxcl8b.1 (ENSDARG00000102299, also known as Cxcl8-l2), require the chemokine receptor Cxcr2 to promote neutrophil chemotaxis (de Oliveira et al., 2015; de Oliveira et al., 2013; Deng et al., 2013; Sarris et al., 2012). It is also known that Cxcl8a, differently from its human counterpart, does not require the zebrafish Cxcr1 receptor and chemoattracts neutrophils essentially via Cxcr2 (Deng et al., 2013). Whether other lineages of chemokine and non-chemokine ligands are chemotactic towards Cxcr1-2 in zebrafish is not currently known.

A cluster of genes that conserves high sequence homology and synteny with the human CXCL9-10-11 gene cluster also exists in zebrafish (Nomiyama et al., 2013; Torraca et al., 2015). Two of these, namely Cxcl11.1 (ENSDARG00000100662) and Cxcl11.6 (ENSDARG00000094706), are infection-inducible and require the chemokine receptor Cxcr3.2, an orthologue of mammalian CXCR3. Similarly to the CXCR3 axes existing in both humans and mice, the receptor Cxcr3.2 (ENSDARG00000041041) induces macrophage recruitment (Torraca et al., 2015). In addition, macrophages and neutrophils in zebrafish express and are mobilised via Cxcr4b (ENSDARG00000041959) (Walters et al., 2010) and this receptor has been shown to cross communicate with the human CXCL12, the ligand of human CXCR4 (Tulotta et al., 2016).

Zebrafish also have a series of other CXC motif chemokines that cannot be unambiguously classified with respect to the primate and rodent counterparts, due to the short sequence and the fast evolution and divergence of chemokine genes (Nomiyama

et al., 2013). The absence of the ELR motif in neutrophil-competent teleost chemokines additionally complicates phylogenetic reconstructions and functional classification. Cxcl18b (ENSDARG00000075045, formerly also known as Cxcl-c1c) is highly induced in zebrafish upon infection with different pathogens and shares sequence similarities and expression patterns with the zebrafish orthologues of both Cxcl8 and Cxcl11 chemokines (48-53% amino acid similarities to Cxcl8a, Cxcl8b.1, Cxcl11.1 and Cxcl11.6) (Jiang et al., 2015; Nomiyama et al., 2013; Stockhammer et al., 2009; van der Vaart et al., 2013). Alignment of Cxcl18b to human CXCL1-2-3-5-6-7-8-9-10-11 chemokines shows 40-48% sequence similarity, with CXCL10 (47.5%) and CXCL8 (47.9%) being the most similar ones in terms of residue conservation.

Like other inflammatory chemokines, c*xcl18b* transcription was found to rely on the activation of the Myd88-dependent innate immunity signalling pathway during the response to *Edwardsiella tarda*, *Mycobacterium marinum (Mm)* and *Salmonella enterica* serovar Typhimurium (Stockhammer et al., 2009; van der Vaart et al., 2013). Recently, it was also demonstrated that Cxcl18b is upregulated in response to treatment with toxic and pro-apoptotic compounds, which indicates this gene as a marker of inflammation in general (Jiang et al., 2015; Jiang et al., 2014). However, the function of Cxcl18b has yet to be elucidated and clarification of its role has an important translational significance, since the zebrafish model is being increasingly used to study chemokine axes, leukocyte biology, and inflammatory processes (Bird and Tafalla, 2015). This study demonstrates that Cxcl18b is an additional neutrophil chemotactic factor. We show that the function of Cxcl18b relies, at least partly on chemokine receptor Cxcr2, and not on Cxcr1 and Cxcr4b. Finally, using a novel reporter line, we show the expression of this chemokine during the pathological inflammation occurring upon mycobacterial infection.

2. Materials and methods

2.1. Zebrafish lines and embryo/larvae handling

Zebrafish were handled in compliance with the local (Leiden University) animal welfare policies and were maintained according to standard protocols (zfin.org). All experiments

in this study were performed on 2 dpf embryos, therefore prior the free feeding stage and did not fall under animal experimentation law according to the EU Animal Protection Directive 2010/63/EU. Embryos were kept in egg water (60 µg/ml sea salt; Sera Marin) at 28.5°C. To prevent pigmentation, embryos were maintained in water supplemented with 0.003% PTU (1-phenyl-2-thiourea, Sigma-Aldrich). For the recruitment assays, neutrophils and macrophages were labelled with the transgenes *Tg(mpx:eGFP^{i114})* or *Tg(mpeg1:Gal4-VP16^{gl24}/UAS-E1b:Kaede^{s1999t})* [in short referred to as *Tg(mpeg1:Gal4/UAS:Kaede)*], respectively (Ellett et al., 2011; Renshaw et al., 2006). For confocal microscopy (Fig. 4), neutrophil and macrophage lines *Tg(lyz:DsRed^{nz50})* (Hall et al., 2007) and *Tg(mpeg1:mCherry-F^{ump2})* (Bernut et al., 2014)were single crossed to the *cxcl18b:eGFP* line (see below). To address chemotactic properties of Cxcl18b via Cxcr4b, mutants (*cxcr4b$^{-/-}$*) and wildtype siblings (*cxcr4b$^{+/+}$*) of *(cxcr4b^{t26035})* (Knaut et al., 2003), crossed into the *Tg(mpx:eGFP^{i114})* background were used.

2.2. Production and verification of recombinant Cxcl18b

The coding sequence for Cxcl18b (ENSDARG00000075045/ENSDART00000111598), generated synthetically (BaseClear), was optimised for expression in *Pichia pastoris*, supplemented with an HA (human influenza haemagglutinin)-tag at the C-terminus and cloned into pPICZα expression vector (Invitrogen, Life Technologies). The expression plasmid was linearised with SacI and transformed into *Pichia pastoris* strain X-33 as described previously (Torraca et al., 2015; Wu and Letchworth, 2004). Successful transformants were selected by resistance to 1000 µg/ml Zeocine. Highly resistant clones were selected for expression efficiency by liquid culturing the isolates in buffered minimal methanol medium (100 mM potassium phosphate buffer pH 6, 1.34% yeast nitrogen base, $4 \cdot 10^{-5}$% biotin, 0.5% methanol, Sigma-Aldrich), for five days at 30ºC/180 rpm, with additional 0.5% methanol supplemented daily. The supernatant of the cultures was probed for anti-HA reactivity on western blot, using a horseradish peroxidase-directly conjugated antibody. (AB_378887, Roche). One clone was selected for large-scale culture. Cxcl18b-HA accumulated in the supernatant was concentrated and purified in PBS by filtration between columns with a cut-off of 50 kDa and 3 kDa (Amicon Ultra

Centrifugal filters, Merck KGaA). Identity and purity of Cxcl18b in the sample was determined by silver staining and by trypsinisation followed by electrospray mass spectrometry analysis, which revealed high quality of the protein and undetectable protein contaminations of the recombinant Cxcl18b with *P. pastoris* proteins (Supplementary Figure **S1**). To obtain a mock control for injections, isolation was performed from the supernatant of non-transformed isogenic *P. pastoris*, cultured in identical condition (with the exception of Zeocine 100 μg/ml present in the starter plate and pre-culture for the transformed isolate). We confirmed chemokine purity and identity by in-solution trypsinisation and electrospray mass spectrometry. Quantification was obtained by BCA-assay (Micro BCATM Protein Assay Kit, Thermo Fisher Scientific, Life Technologies), the protein concentration assessed by the assay in the mock is subtracted from the total Cxcl18b protein concentration.

2.3. Recruitment assays

Cxcl18b, Cxcl8a or mock (produced as described above), were diluted in PBS to the desired concentration (0.2-2 ng/nl) and injected (1 nl) into the hindbrain ventricle of 2 dpf embryos. Prior and during injections, embryos were anaesthetised in egg water medium containing 0.02% buffered Tricaine (3-aminobenzoic acid ethyl ester; Sigma-Aldrich). The embryos were fixed (O/N) at 3 h post injection (hpi) in PBSTx (1 × PBS supplemented with 0.8% Triton X-100, Sigma-Aldrich) containing 4% paraformaldehyde. Subsequently, the embryos were washed in PBS and the fluorescently labelled cells within the hindbrain perimeter were counted (blinded) using a Leica MZ16FA fluorescence stereomicroscope.

2.4. Pharmacological inhibition of Cxcr2

For the Cxcr2 inhibition assays, we followed and adapted the protocol used by (de Oliveira et al., 2013). Briefly, 2 dpf larvae were preincubated for 1 h at 28.5°C in presence or absence of SB225002 (Sigma-Aldrich), a selective nonpeptide inhibitor of human CXCR2, at a concentration of 5 μM in egg water. Since the compound is initially suspended in DMSO, the control group was exposed to the same concentration of DMSO (Sigma-Aldrich) alone (0.05%) as in the SB225002 group. Upon injection, embryos were returned and maintained in SB225002 or vehicle treatment until they were fixed (3 hpi) in 4% paraformaldehyde in PBSTx O/N.

2.5. Knockdown of Cxcr1

3 nl of 75 μM *cxcr1* morpholino (5′-TGTCAGGATACTAAACTTACCAGTC-3′, targeting exon1-intron 1 splicing site, Gene tools) or the same volume and concentration of a standard control morpholino (5′-CCTCTTACCTCAGTTACAATTTATA-3′, Gene tools) were injected at 1 cell stage in zebrafish fertilised eggs, according to previous reports (Deng et al., 2013).

2.6. Cloning of *cxcl18b* promoter and construction of *Tg(cxcl18b:eGFP)* reporter line

3.04 kb of *cxcl18b* promoter immediately proximal to the transcriptional start were amplified from genomic DNA derived from a pool of AB/TL embryos, using the following amplification primers: *XhoI-Cxcl18bFw:* 5′-GGGCCCCTCGAGGTCTCCTCATGCATTGACTAC-3′ and *BamHI-Cxcl18bRv:* 5′-GGGCCCGGATCCAATTGCTGCAAACTATATGTAGG-3′. The PCR resulted in a single band on gel electrophoresis at the expected molecular weight. The primers supplemented the sequence with a unique XhoI site at the 5′ end, a unique BamHI site at the 3′ end and with exceeding 5′-GGGCCC-3′ extremities preceding both restriction sites to facilitate digestion. XhoI and BamHI extremities were activated by double enzymatic digestion to permit cloning into a custom-adapted pTol2^{+} destination vector, upstream of the eGFP coding sequence. Briefly, the destination vector was derived from *pTol2*$^{+}$*/coro-1a:eGFP-SV40pA* vector, previously described and kindly provided by the Wen lab (Li et al., 2012). The *7.03* kb *coro-1a* promoter sequence was fully removed by double restriction and gel extraction and replaced by a multiple cloning site, containing a BamHI proximal to the eGFP transcription start and an XhoI site more distally. Both vector and *XhoI-cxcl18b-BamHI* constructs where BamHI/XhoI digested and ligated together to obtain *pTol2*$^{+}$*/cxcl18b:eGFP-SV40pA*. The plasmid was purified and injected into zebrafish fertilised eggs together with the Tol2-transposase mRNA, according to previous reports (Ellett et al., 2011). Several founders were identified and appeared very similar in basal eGFP expression. One eGFP-positive founder was selected, outcrossed to AB/TL and the positive F1 offspring was raised to adulthood.

2.7. *M. marinum* infection and image acquisition

Tg(cxcl18b:eGFP) embryos were injected with 200 CFU of mCrimson-labelled *M. marinum* strain M by the caudal vein injection route (Fig. 3) or with 50 CFU via the trunk injection route (Fig. 4). Bacteria were handled, prepared and injected as previously described (Benard et al., 2012; Torraca et al., 2015). Stereo-fluorescence images in Fig. 3 were taken with a Leica MZ16FA fluorescence stereomicroscope connected to a Leica DFC420C camera (Leica Microsystems). Confocal images were acquired with a Leica TCS SPE microscope equipped with a HCX APO L U-V-I 40×/WATER objective (Leica Microsystems) (Fig. 4A–F) or with Zeiss Observer 6.5.32 laser-scanning microscope equipped with Plan-Neofluar 40×/0.9 Imm corr objective (Carl Zeiss) (Fig. 4G–L).

2.8. Statistical analysis

All data were analysed using GraphPad Prism 5 (GraphPad Software). For comparison between two groups (Fig. 1), a Mann-Whitney test was used. For comparisons between more than two groups (Fig. 2) a Kruskal-Wallis test was used, followed by Sidak's multiple comparisons post-hoc test for selected groups. Significance (*P*-value) is indicated as: ns (non-significant); * ($P < 0.05$); ** ($P < 0.01$); *** ($P < 0.001$); **** ($P < 0.0001$). Error bars in all the graphs are mean ± s.e.m.

3. Results

3.1. Cxcl18b induces chemotaxis of neutrophils, but not macrophages

In order to study the chemotactic properties of Cxcl18b, we produced a HA (human influenza haemagglutinin)-tagged recombinant Cxcl18b using a yeast (*Pichia pastoris*) expression system and we confirmed identity and purity of the isolated protein by electrospray mass spectrometry analysis (Suppl. Fig. S1). To study the function of Cxcl18b, the isolated chemokine was injected into the hindbrain ventricle of embryos at 2 dpf (days post fertilisation), in neutrophil-specific (*mpx:eGFP*-positive cells) or macrophage-specific (*mpeg1:Gal4/UAS:Kaede*-positive cells) transgenic reporter backgrounds (Ellett et al., 2011; Renshaw et al., 2006). Embryos were fixed 3 h post injection (hpi). As a negative control for injections (mock), the supernatant of a non-

transformed *Pichia pastoris* culture was processed with the same purification procedure. Injection of either 0.2 or 2 ng of purified recombinant Cxcl18b elicited significantly higher mobilisation of neutrophils when compared to mock, while it did not impact on macrophage recruitment (Fig. 1), indicating that Cxcl18b has chemotactic specificity toward neutrophils. Injection of either 0.2 or 2 ng of Cxcl18b did not affect the overall level of recruitment in a dose-dependent manner, suggesting that receptor saturation may have occurred or that stimulation with larger doses is no longer able to increase the frequency and/or speed by which the neutrophils are polarizing towards the source of the signal. It was in fact shown that neutrophil chemotactic migration is elicited by imposing an orthotactic bias to the cell random motility according to the direction of the source (Sarris et al., 2012).

3.2. Cxcl18b requires Cxcr2 receptor, but not Cxcr1 and Cxcr4b, for efficient recruitment of neutrophils

The chemokine receptor Cxcr2/CXCR2 is a key controller of neutrophil chemotaxis in both teleosts and mammalian species (de Oliveira et al., 2013; Deng et al., 2013; Russo et al., 2014; Wolf et al., 1998). In mammals, activation of neutrophil migration via CXCR2 can be obtained by stimulation with a wide spectrum of inflammatory CXC chemokines, including CXCL1-2-3-5-6-7-8(Ahuja and Murphy, 1996; Pelus et al., 2002; Wolf et al., 1998). Hence, CXCR2 represents a ligand-promiscuous, but neutrophil-specific, receptor. In zebrafish, 2 functional Cxcl8 ligands of Cxcr2, namely Cxcl8a and Cxcl8b.1, have been identified (de Oliveira et al., 2013; Deng et al., 2013; Nomiyama et al., 2013) . However, considering the capability of the mammalian CXCR2 to accommodate a multiplicity of chemokines, it is very likely that also in zebrafish other CXC chemokines are redundant with Cxcl8 ligands. Therefore, we hypothesised that the neutrophil chemotactic properties of Cxcl18b might also be exerted by activation of Cxcr2. To test this hypothesis we pharmacologically inhibited Cxcr2 with SB225002, a non-peptide inhibitor that can suppress both mammalian and zebrafish CXCR2 activity against its ligands, such as CXCL1 and CXCL8 (de Oliveira et al., 2013; White et al., 1998). As a positive control, zebrafish Cxcl8a, isolated with a comparable method (Torraca et al., 2015), was used, since it was previously

demonstrated that blockade of Cxcr2 with SB225002 can affect Cxcl8-dependent chemotaxis in zebrafish (de Oliveira et al., 2013). Cxcl8a and Cxcl18b elicited increased recruitment of neutrophils in control (DMSO vehicle-treated) groups and a significantly diminished chemotactic potency in SB225002-treated groups, which indicated that both Cxcl8a and Cxcl18b require Cxcr2 to mediate optimal neutrophil chemotaxis (Fig. 2A). However, the chemotactic capability of Cxcl8a was more severely suppressed by the drug treatment, as compared to the effect exerted by the same treatment on Cxcl18b chemotaxis, since this could still recruit more neutrophils than mock in Cxcr2-depleted condition.

We also tested the activity of Cxcl18b under condition of *cxcr1* morpholino knockdown and in a *cxcr4b* mutant line, since these other two receptors are also expressed by zebrafish neutrophils (Deng et al., 2013; Walters et al., 2010). However, Cxcl18b did not display significantly diminished chemoattractant power in *cxcr1* or *cxcr4b* depleted conditions, indicating that these receptors are dispensable for Cxcl18b sensing (Fig. 2B–C). To address whether redundant function between Cxcr1 and Cxcr2 might explain that *cxcr1* morpholino injection did not impair neutrophil recruitment, we blocked Cxcr1/2 signalling by *cxcr1* knockdown and simultaneous Cxcr2 pharmacological inhibition. Simultaneous blockade of Cxcr1 and Cxcr2 significantly reduced neutrophil recruitment, but suppression of neutrophil chemotaxis did not significantly differ from that evoked by Cxcr2 inhibition alone (Fig. 2A–B).

3.3. A *Tg(cxcl18b:eGFP)* reporter lines labels mycobacterial-induced inflammation

Since previous expression studies indicated that Cxcl18b (formerly known as Cxcl-c1c) is induced in response to several bacterial infections (Stockhammer et al., 2009; van der Vaart et al., 2013), we constructed a *Tg(cxcl18b:eGFP)* reporter line to visualise and longitudinally follow the expression pattern of *cxcl18b in vivo*. To validate inflammation-dependent induction of the reporter line, we injected embryos with *Mycobacterium marinum* (*Mm*), a fish pathogen which leads to the formation of granulomatous lesions in the zebrafish species and is widely used as a surrogate model for tuberculosis (Davis et al., 2002). These inflammatory lesions consist of immune cell

aggregates that have migrated and collected bacteria at the infection focus. The initial stages of granuloma formation mostly consist of macrophages, while neutrophils are mostly recruited at a more advanced stage. Granulomas in the zebrafish embryonic/larval model form without requiring the presence of adaptive immune cells, as these lesions can be generated at developmental stages that anticipate ontogenesis of lymphocytes (Davis et al., 2002). When *Tg(cxcl18b:eGFP)* embryos were challenged with *Mm*, the *cxcl18b*-driven eGFP accumulated in the areas where initial aggregates were forming (Fig. 3), consistent with previous evidence reported by transcriptomic studies (van der Vaart et al., 2013). At 36 hpi, cells residing in the caudal haematopoietic tissue and endothelial cells appeared to upregulate the transgene. (Fig. 3E–F). As the infection progressed, the expression of the reporter continued to accumulate at the nascent granulomas in the cells surrounding the lesion. However, confocal imaging of the infected larvae indicates that the infected cells are not the main producers of *cxcl18b*, rather this is produced by non-infected cells in the immediate surrounding tissue (Fig. 4A–F). These *cxcl18b*-expressing cells localised in tight proximity to the cells where most of the infection was residing, participating in the formation of the nascent granulomatous aggregates. At 3-4 dpi (days post infection), highly *cxcl18b*-expressing cells could be found within the granuloma lesion. Considering the capability of some of the Cxcl18b+ cells to emit long dendrites (Fig. 4C–F), we investigated whether these cells could represent uninfected phagocytes (macrophages and neutrophils). Therefore, we crossed the *Tg(cxcl18b:eGFP)* transgenic line with *Tg(lyz:DsRed)* or *Tg(mpeg1:mCherry-F)* lines and infected the offspring with Mm-mCrimson to induce *cxcl18b:eGFP* expression. As expected, the infection resided essentially in cxcl18b-negative cells, although the nascent granuloma aggregates contained several cxcl18b-positive cells. Strikingly, the *cxcl18b* transgene expression did not overlap with *lyz* and *mpeg1* transgenes, indicating that Cxcl18b is expressed by non-phagocytic cells that participate in the granuloma aggregate. Since we identified Cxcl18b as a potent neutrophil chemoattractant and neutrophils are known to be attracted to the granulomatous aggregates (Yang et al., 2012), Cxcl18b-producing non-phagocytic cells that compose the granuloma stroma might be important to drive neutrophil recruitment to the mycobacterial infection foci.

4. Discussion

Our study reports that the zebrafish chemokine Cxcl18b, a reliable marker of inflammation, displays expression patterns and chemotactic properties towards neutrophils, similar to those of the zebrafish Cxcl8 paralogues, as both Cxcl8 chemokines and Cxcl18b require the chemokine receptor/neutrophil marker Cxcr2 to mediate an optimal neutrophil emigration (de Oliveira et al., 2013). Our study therefore indicates that, like in mammalian species, the zebrafish Cxcr2 is a promiscuous receptor, able to respond to a variety of CXC ligands (Russo et al., 2014). However, while Cxcl8a heavily relies on Cxcr2 activity to induce chemotaxis, Cxcl18b can still elicit significant (although diminished) neutrophil recruitment in Cxcr2-depleted conditions, indicating that another neutrophil receptor can mediate residual Cxcl18b chemotaxis in Cxcr2-blocked conditions. We excluded the possibility that this receptor may be Cxcr4b or Cxcr1, other two chemokine receptors expressed by the neutrophil lineage which can affect neutrophil chemotaxis in zebrafish and/or mammals (Stillie et al., 2009; Walters et al., 2010), since Cxcl18b could still elicit normal recruitment of neutrophil in a *cxcr4b* mutant line or in *cxcr1* knockdown conditions. These data are in line with previous studies in zebrafish that demonstrated that Cxcr1 is also not required to sense the zebrafish Cxcl8a and Cxcl8b.1 chemokines that essentially recruit via Cxcr2 (de Oliveira et al., 2015; de Oliveira et al., 2013; Deng et al., 2013), and with the fact that Cxcr4b elicits cell recruitment via the Cxcl12a ligand (Valentin et al., 2007)., and with the fact that Cxcr4b elicits cell recruitment via the Cxcl12a ligand The residual recruitment of neutrophils upon Cxcl18b injection can be explained either with the existence of another neutrophil receptor that contributes to Cxcl18b-mediated recruitment, or with the possibility that the Cxcr2 inhibitor may not have completely suppressed Cxcr2 function, which could lead to some residual neutrophil recruitment.

In this study, we have also constructed a *cxcl18b* reporter line that can be used to further investigate what cell types are involved in the production of the Cxcl18b neutrophil-chemotactic cue. Our analysis of the *cxcl18b* transgene expression indicates that non-

phagocytic cells at the infection site are responsible for *cxcl18b* expression in response to *Mm* bacterial challenge. This observation also suggests an important contribution of stromal cells in the granuloma microenvironment to the development of inflammation. A study investigating *cxcl8a* and *cxcl8b.1* expression in the gut, demonstrated that (in physiological condition) *cxcl8a* is largely expressed by non-immune (epithelial) cells with a mechanism that requires adaptive immune signalling (Brugman et al., 2014). On the other hand the same study also demonstrated that, in the inflammatory gut, induction of both *cxcl8a* and *cxcl8b.1* did not require adaptive immune signalling, which is similar to our finding that *cxcl18b* can be induced in stromal cells of the granulomas at developmental stages that anticipate ontogenesis of the adaptive immunity. A better understanding of responses in the granuloma microenvironment is particularly relevant in view of the emerging role of inflammation in the pathogenesis of tuberculosis, with several recent studies emphasising the need for a well-balanced inflammatory response in order to provide protective functions yet prevent pathological consequences (Dorhoi and Kaufmann, 2014; Matty et al., 2015).

In a recent study, *cxcl18b* was the most upregulated chemoattractant detected at 4 h post tail fin amputations (Chatzopoulou et al., 2016), indicating that *cxcl18b* is also induced upon sterile acute inflammation. Notably, in this study the expression of *cxcl18b* was fully suppressed by treatment with the glucocorticoid beclomethasone. Treatment with this anti-inflammatory drug coincided with the abolishment of neutrophil recruitment to the wound, while it did not affect macrophage recruitment (Chatzopoulou et al., 2016). Given our evidence that Cxcl18b is a potent and neutrophil-specific chemotactic cue, neutrophil chemotaxis might have been impaired by beclomethasone treatment owing to significant suppression of *cxcl18b* induction. Previous studies performed in a similar model showed that, at 1 h post wounding (hpw), the two zebrafish *cxcl8a* and *cxcl8b.1* genes were also significantly induced. While induction of *cxcl18b* was not addressed at 1 hpw, induction of *cxcl8a* and *cxcl8b.1* was found to be very transient and significantly dropped down at 4 hpw (de Oliveira et al., 2013). Similarly, in another report investigating infiltration of neutrophils in physiological and inflamed gut, *cxcl8a* and *cxcl8b.1* were found to be differentially regulated by alternative signalling machineries

and to be highly dynamic over time (Brugman et al., 2014). Taken together, these studies suggest that Cxcl8a-Cxcl8b.1 and Cxcl18b might represent differently timed chemotactic cues which may be responsible for the recruitment of different waves (or different subpopulations) of neutrophils during homoeostatic, acute, and chronic inflammatory responses (Brugman et al., 2014; de Oliveira et al., 2013). Further investigations using the zebrafish model might therefore help to investigate *in vivo* the biological significance underlying the existence of different Cxcl8-like chemokines. Understanding to what extent Cxcl18b is redundant with Cxcl8 isoforms and whether the two clades of chemokines also display specific functions in the regulation of the inflammatory response could also shed light on the divergences and/or convergences existing between fish and mammalian chemokine axes and on the evolutionary diversification of chemokine ligands.

Acknowledgements

We thank Marco Siderius and Jan-Paul Bebelman (VU University, Amsterdam) for *P. pastoris* clone design and recombinant protein production, Bobby Florea for the help with mass spectrometry validation of recombinant Cxcl18b, and Julien Rougeot for providing the custom-adapted pTol2^{+} destination vector. We thank all members of the fish facility team for zebrafish care. We also acknowledge Monica Varela for valuable suggestions and for critically reading the manuscript.

Funding

This work was supported by the European Marie-Curie Initial Training Network FishForPharma (contract number PITN-GA-2011-289209).

Authorship

VT and AHM designed the study and wrote the manuscript. VT, NAO, and ATT performed the experiments and analysed the data. The manuscript was approved and read by all the co-authors.

Figure legends

Fig. 1. Cxcl18b exerts a neutrophil-specific chemoattraction. Purified Cxcl18b-HA (0.2 or 2 ng) or mock (isovolumetric) were injected in the hindbrain of 2 dpf zebrafish embryos from *Tg(mpx:eGFP)* or *Tg(mpeg1:Gal4/UAS:Kaede)* lines. Samples were collected at 3 hpi. While Cxcl18b did not significantly chemoattract macrophages more than mock at both concentrations (B,D), Cxcl18b injection induced an increased infiltration of neutrophils to the hindbrain (A,C), indicating the chemotactic capability of this ligand towards neutrophils. Each data point represents an individual embryo. Data are cumulated from 4 (A), 2 (B–C) or 1 (D) replicates.

Fig. 2. Pharmacological inhibition of CXCR2, but not *cxcr1* knockdown or homozygote mutation of *cxcr4b*, attenuates neutrophil recruitment to Cxcl18b local injections. A. Injections in the hindbrain of Cxcl18b (2 ng) or Cxcl8a (0.5 ng) were performed as in Fig. 1. Pharmacological inhibition of Cxcr2 by bath exposure to 5 μM SB225002 affected the chemoattraction of neutrophils to both Cxcl8a and Cxcl18b but did not entirely suppress the chemotactic response to Cxcl18b, suggesting that Cxcl18b could be sensed by an additional receptor. B. Morpholino knockdown of *cxcr1* did not affect neutrophil migration to Cxcl18b and did not synergise with Cxcr2 inhibition, as Cxcr1/2 deficient embryos still displayed residual recruitment when compared to mock-injected controls. C. *cxcr4b* null mutant embryos did not display impaired neutrophil recruitment to Cxcl18b, indicating that this receptor is not required for the Cxcl18b-dependent chemotaxis of neutrophils. Data are cumulated from 2 (A–B) or 1 (C) replicates.

Fig. 3. *cxcl18b:eGFP* is expressed by the tissue surrounding *M. marinum* infection sites. Injections of approximately 200 CFU of *M. marinum* M-mCrimson (*Mm*) via the caudal vein (A-B and E-F), but not mock injection (2% PVP in PBS, C-D and G-H) induced expression of the *cxcl18b-eGFP* transgene in the infected areas, especially localised around the sites of bacterial growth. Images were taken at 36 hpi. Scale bars: 100 μm.

Fig. 4. *cxcl18b:eGFP* is expressed by non-infected cells accumulated at the nascent granuloma. A-F. During the formation of granulomas, the cells that express high levels of *cxcl18b-eGFP* consist predominantly of uninfected cells that participate in the cell aggregates initiating the granuloma. Phenotypic inspection shows that some of these cells can emit long protrusions (arrow in C). G-L. Cxcl18b-expressing cells do not represent phagocytic cells since this marker does not overlap with established neutrophil and macrophage markers l*yz* (G–I) and *mpeg1* (J–L). Images are representative of granulomas forming at 3 dpi (A–F) or 4 dpi (G–L). A-B are multiple z-stack maximum projections, C-L are split channels and overlay of an individual optical layer. In G-L outlines of green and red cells are marked with dashed lines of the corresponding colour. Scale bars: 10 μm. (For interpretation of the references to colour in this figure legend, the reader is referred to the web version of this article.)
caption

Supplementary figure legend

Suppl. Fig. S1. Cxcl18b recombinant protein production. A. Western blot analysis of the supernatant derived from eight (#1-#8) isolates of *P. pastoris* transformed with Cxcl18b-HA expression vector. The protein was visualised by a HRP-conjugated anti-HA antibody. Lanes marked as ctr refer to the supernatant of two non-transformed isolates. The expected molecular weight of Cxcl18b-HA is 11.5 kDa. However, in the western blot analysis Cxcl18b displayed two bands, one at about 20 kDa and one at about 40 kDa. The 40 kDa band represents most likely a dimer of the 20 kDa product. Increased molecular weight of Cxcl18b as compared to expectation can be explained by glycosylation, difference in salinity/ionic force between the *P. pastoris* culture supernatants and the reference protein ladder (L), and high protein concentration in the samples that may delay electrophoretic run. Isolate #8, which appeared to produce the highest levels of recombinant protein, was selected for purification and confirmation by mass spectrometry. B-C. Electrospray mass spectrometry analysis of trypsinised Cxcl18b-HA. Virtually all the peptides derived from trypsinisation of Cxcl18b (peptides 1–11) could be detected. Short stretches of the protein could not be identified with statistical significance, because of the high frequency of trypsin digestion sites (.K or.R) on those protein parts (predicted peptides ARR, A, R, PNCD consist of ≤4 residues and are too short for univocal identification). No other zebrafish or *Pichia pastoris* proteins were significantly indicated by the mass spectrometry analysis of purified Cxcl18b. Bars in black in B show the sequence covered by mass spectrometry analysis. The sequence underlined in blue indicates the C-terminal HA tag, used for western blot readout in A. Table of peptide statistics in C was elaborated via Mascott analysis of the Cxcl18b-HA spectrum.

References

Ahuja, S.K., Murphy, P.M., 1996. The CXC chemokines growth-regulated oncogene (GRO) alpha, GRObeta, GROgamma, neutrophil-activating peptide-2, and epithelial cell-derived neutrophil-activating peptide-78 are potent agonists for the type B, but not the type A, human interleukin-8 receptor. The Journal of biological chemistry 271, 20545-20550.

Benard, E.L., van der Sar, A.M., Ellett, F., Lieschke, G.J., Spaink, H.P., Meijer, A.H., 2012. Infection of zebrafish embryos with intracellular bacterial pathogens. Journal of visualized experiments : JoVE.

Bernhagen, J., Krohn, R., Lue, H., Gregory, J.L., Zernecke, A., Koenen, R.R., Dewor, M., Georgiev, I., Schober, A., Leng, L., Kooistra, T., Fingerle-Rowson, G., Ghezzi, P., Kleemann, R., McColl, S.R., Bucala, R., Hickey, M.J., Weber, C., 2007. MIF is a noncognate

ligand of CXC chemokine receptors in inflammatory and atherogenic cell recruitment. Nat Med 13, 587-596.
Bernut, A., Herrmann, J.L., Kissa, K., Dubremetz, J.F., Gaillard, J.L., Lutfalla, G., Kremer, L., 2014. Mycobacterium abscessus cording prevents phagocytosis and promotes abscess formation. Proceedings of the National Academy of Sciences of the United States of America 111, E943-952.
Bird, S., Tafalla, C., 2015. Teleost Chemokines and Their Receptors. Biology (Basel) 4, 756-784.
Brugman, S., Witte, M., Scholman, R.C., Klein, M.R., Boes, M., Nieuwenhuis, E.E., 2014. T lymphocyte-dependent and -independent regulation of Cxcl8 expression in zebrafish intestines. Journal of immunology 192, 484-491.
Cai, Z., Gao, C., Zhang, Y., Xing, K., 2009. Functional characterization of the ELR motif in piscine ELR+CXC-like chemokine. Mar Biotechnol (NY) 11, 505-512.
Chatzopoulou, A., Heijmans, J.P., Burgerhout, E., Oskam, N., Spaink, H.P., Meijer, A.H., Schaaf, M.J., 2016. Glucocorticoid-Induced Attenuation of the Inflammatory Response in Zebrafish. Endocrinology 157, 2772-2784.
Clark-Lewis, I., Dewald, B., Geiser, T., Moser, B., Baggiolini, M., 1993. Platelet factor 4 binds to interleukin 8 receptors and activates neutrophils when its N terminus is modified with Glu-Leu-Arg. Proceedings of the National Academy of Sciences of the United States of America 90, 3574-3577.
Davis, J.M., Clay, H., Lewis, J.L., Ghori, N., Herbomel, P., Ramakrishnan, L., 2002. Real-time visualization of mycobacterium-macrophage interactions leading to initiation of granuloma formation in zebrafish embryos. Immunity 17, 693-702.
de Oliveira, S., Lopez-Munoz, A., Martinez-Navarro, F.J., Galindo-Villegas, J., Mulero, V., Calado, A., 2015. Cxcl8-l1 and Cxcl8-l2 are required in the zebrafish defense against Salmonella Typhimurium. Dev Comp Immunol 49, 44-48.
de Oliveira, S., Reyes-Aldasoro, C.C., Candel, S., Renshaw, S.A., Mulero, V., Calado, A., 2013. Cxcl8 (IL-8) mediates neutrophil recruitment and behavior in the zebrafish inflammatory response. Journal of immunology (Baltimore, Md. : 1950) 190, 4349-4359.
Deng, Q., Sarris, M., Bennin, D.A., Green, J.M., Herbomel, P., Huttenlocher, A., 2013. Localized bacterial infection induces systemic activation of neutrophils through Cxcr2 signaling in zebrafish. J Leukoc Biol 93, 761-769.
Dorhoi, A., Kaufmann, S.H., 2014. Perspectives on host adaptation in response to Mycobacterium tuberculosis: modulation of inflammation. Semin Immunol 26, 533-542.
Ellett, F., Pase, L., Hayman, J.W., Andrianopoulos, A., Lieschke, G.J., 2011. mpeg1 promoter transgenes direct macrophage-lineage expression in zebrafish. Blood 117, e49-56.
Gaggar, A., Jackson, P.L., Noerager, B.D., O'Reilly, P.J., McQuaid, D.B., Rowe, S.M., Clancy, J.P., Blalock, J.E., 2008. A novel proteolytic cascade generates an extracellular matrix-derived chemoattractant in chronic neutrophilic inflammation. Journal of immunology (Baltimore, Md. : 1950) 180, 5662-5669.
Hall, C., Flores, M.V., Storm, T., Crosier, K., Crosier, P., 2007. The zebrafish lysozyme C promoter drives myeloid-specific expression in transgenic fish. BMC Dev Biol 7, 42.
Harvie, E.A., Huttenlocher, A., 2015. Neutrophils in host defense: new insights from zebrafish. J Leukoc Biol 98, 523-537.
Hruscha, A., Schmid, B., 2015. Generation of zebrafish models by CRISPR /Cas9 genome editing. Methods Mol Biol 1254, 341-350.
Jiang, J., Wu, S., Wang, Y., An, X., Cai, L., Zhao, X., Wu, C., 2015. Carbendazim has the potential to induce oxidative stress, apoptosis, immunotoxicity and endocrine disruption during zebrafish larvae development. Toxicol In Vitro 29, 1473-1481.

Jiang, J., Wu, S., Wu, C., An, X., Cai, L., Zhao, X., 2014. Embryonic exposure to carbendazim induces the transcription of genes related to apoptosis, immunotoxicity and endocrine disruption in zebrafish (Danio rerio). Fish Shellfish Immunol 41, 493-500.
Knaut, H., Werz, C., Geisler, R., Nusslein-Volhard, C., Tubingen Screen, C., 2003. A zebrafish homologue of the chemokine receptor Cxcr4 is a germ-cell guidance receptor. Nature 421, 279-282.
Mathias, J.R., Dodd, M.E., Walters, K.B., Yoo, S.K., Ranheim, E.A., Huttenlocher, A., 2009. Characterization of zebrafish larval inflammatory macrophages. Dev Comp Immunol 33, 1212-1217.
Matty, M.A., Roca, F.J., Cronan, M.R., Tobin, D.M., 2015. Adventures within the speckled band: heterogeneity, angiogenesis, and balanced inflammation in the tuberculous granuloma. Immunol Rev 264, 276-287.
Mukaida, N., 2003. Pathophysiological roles of interleukin-8/CXCL8 in pulmonary diseases. Am J Physiol Lung Cell Mol Physiol 284, L566-577.
Nomiyama, H., Osada, N., Yoshie, O., 2013. Systematic classification of vertebrate chemokines based on conserved synteny and evolutionary history. Genes Cells 18, 1-16.
Pelus, L.M., Horowitz, D., Cooper, S.C., King, A.G., 2002. Peripheral blood stem cell mobilization. A role for CXC chemokines. Crit Rev Oncol Hematol 43, 257-275.
Renshaw, S.A., Loynes, C.A., Trushell, D.M., Elworthy, S., Ingham, P.W., Whyte, M.K., 2006. A transgenic zebrafish model of neutrophilic inflammation. Blood 108, 3976-3978.
Russo, R.C., Garcia, C.C., Teixeira, M.M., Amaral, F.A., 2014. The CXCL8/IL-8 chemokine family and its receptors in inflammatory diseases. Expert Rev Clin Immunol 10, 593-619.
Sarris, M., Masson, J.B., Maurin, D., Van der Aa, L.M., Boudinot, P., Lortat-Jacob, H., Herbomel, P., 2012. Inflammatory chemokines direct and restrict leukocyte migration within live tissues as glycan-bound gradients. Current biology : CB 22, 2375-2382.
Stillie, R., Farooq, S.M., Gordon, J.R., Stadnyk, A.W., 2009. The functional significance behind expressing two IL-8 receptor types on PMN. J Leukoc Biol 86, 529-543.
Stockhammer, O.W., Zakrzewska, A., Hegedus, Z., Spaink, H.P., Meijer, A.H., 2009. Transcriptome profiling and functional analyses of the zebrafish embryonic innate immune response to Salmonella infection. Journal of immunology (Baltimore, Md. : 1950) 182, 5641-5653.
Tanino, Y., Coombe, D.R., Gill, S.E., Kett, W.C., Kajikawa, O., Proudfoot, A.E., Wells, T.N., Parks, W.C., Wight, T.N., Martin, T.R., Frevert, C.W., 2010. Kinetics of chemokine-glycosaminoglycan interactions control neutrophil migration into the airspaces of the lungs. Journal of immunology (Baltimore, Md. : 1950) 184, 2677-2685.
Torraca, V., Cui, C., Boland, R., Bebelman, J.P., van der Sar, A.M., Smit, M.J., Siderius, M., Spaink, H.P., Meijer, A.H., 2015. The CXCR3-CXCL11 signaling axis mediates macrophage recruitment and dissemination of mycobacterial infection. Dis Model Mech 8, 253-269.
Torraca, V., Masud, S., Spaink, H.P., Meijer, A.H., 2014. Macrophage-pathogen interactions in infectious diseases: new therapeutic insights from the zebrafish host model. Dis Model Mech 7, 785-797.
Tulotta, C., Stefanescu, C., Beletkaia, E., Bussmann, J., Tarbashevich, K., Schmidt, T., Snaar-Jagalska, B.E., 2016. Inhibition of signaling between human CXCR4 and zebrafish ligands by the small molecule IT1t impairs the formation of triple-negative breast cancer early metastases in a zebrafish xenograft model. Dis Model Mech 9, 141-153.
Valentin, G., Haas, P., Gilmour, D., 2007. The chemokine SDF1a coordinates tissue migration through the spatially restricted activation of Cxcr7 and Cxcr4b. Current biology : CB 17, 1026-1031.

Van Damme, J., Decock, B., Conings, R., Lenaerts, J.P., Opdenakker, G., Billiau, A., 1989. The chemotactic activity for granulocytes produced by virally infected fibroblasts is identical to monocyte-derived interleukin 8. Eur J Immunol 19, 1189-1194.
van der Vaart, M., van Soest, J.J., Spaink, H.P., Meijer, A.H., 2013. Functional analysis of a zebrafish myd88 mutant identifies key transcriptional components of the innate immune system. Dis Model Mech 6, 841-854.
Walters, K.B., Green, J.M., Surfus, J.C., Yoo, S.K., Huttenlocher, A., 2010. Live imaging of neutrophil motility in a zebrafish model of WHIM syndrome. Blood 116, 2803-2811.
Weathington, N.M., van Houwelingen, A.H., Noerager, B.D., Jackson, P.L., Kraneveld, A.D., Galin, F.S., Folkerts, G., Nijkamp, F.P., Blalock, J.E., 2006. A novel peptide CXCR ligand derived from extracellular matrix degradation during airway inflammation. Nat Med 12, 317-323.
White, J.R., Lee, J.M., Young, P.R., Hertzberg, R.P., Jurewicz, A.J., Chaikin, M.A., Widdowson, K., Foley, J.J., Martin, L.D., Griswold, D.E., Sarau, H.M., 1998. Identification of a potent, selective non-peptide CXCR2 antagonist that inhibits interleukin-8-induced neutrophil migration. The Journal of biological chemistry 273, 10095-10098.
Wolf, M., Delgado, M.B., Jones, S.A., Dewald, B., Clark-Lewis, I., Baggiolini, M., 1998. Granulocyte chemotactic protein 2 acts via both IL-8 receptors, CXCR1 and CXCR2. Eur J Immunol 28, 164-170.
Wu, S., Letchworth, G.J., 2004. High efficiency transformation by electroporation of Pichia pastoris pretreated with lithium acetate and dithiothreitol. Biotechniques 36, 152-154.
Yang, C.T., Cambier, C.J., Davis, J.M., Hall, C.J., Crosier, P.S., Ramakrishnan, L., 2012. Neutrophils exert protection in the early tuberculous granuloma by oxidative killing of mycobacteria phagocytosed from infected macrophages. Cell host & microbe 12, 301-312.
Zlotnik, A., Yoshie, O., 2012. The chemokine superfamily revisited. Immunity 36, 705-716.

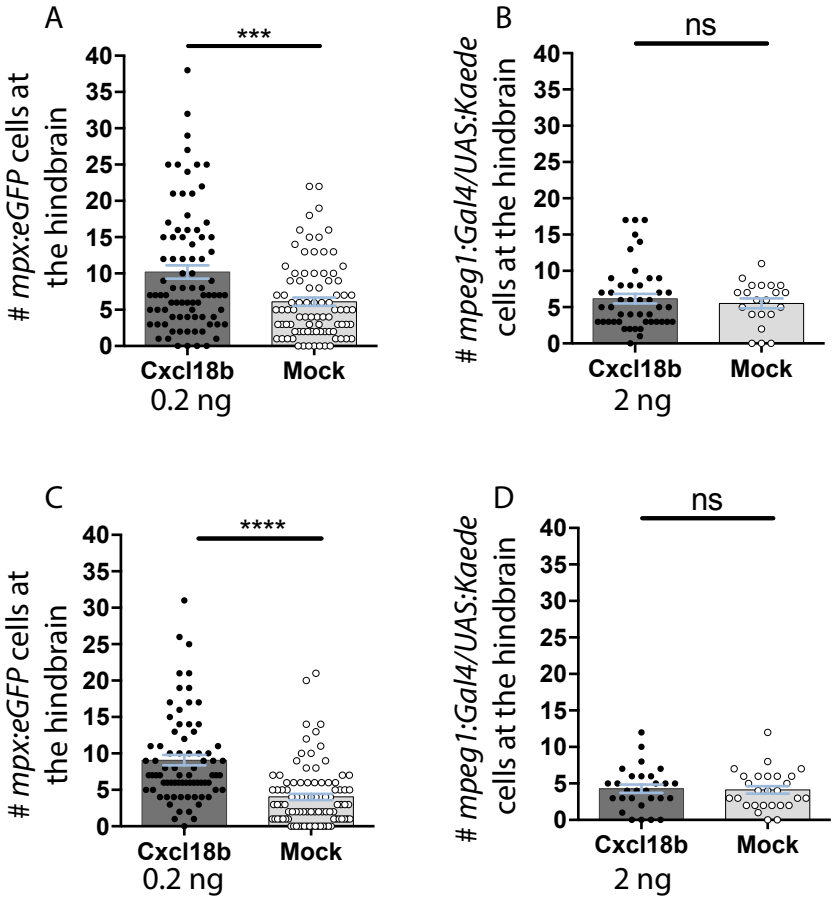
A
***
mpx:eGFP cells at the hindbrain
40
35
30
25
20
15
10
5
0
Cxcl18b
Mock
0.2 ng
B
ns
mpeg1:Gal4/UAS:Kaede cells at the hindbrain
Cxcl18b
Mock
2 ng
C
****
mpx:eGFP cells at the hindbrain
Cxcl18b
Mock
0.2 ng
D
ns
mpeg1:Gal4/UAS:Kaede cells at the hindbrain
Cxcl18b
Mock
2 ng

Figure 1

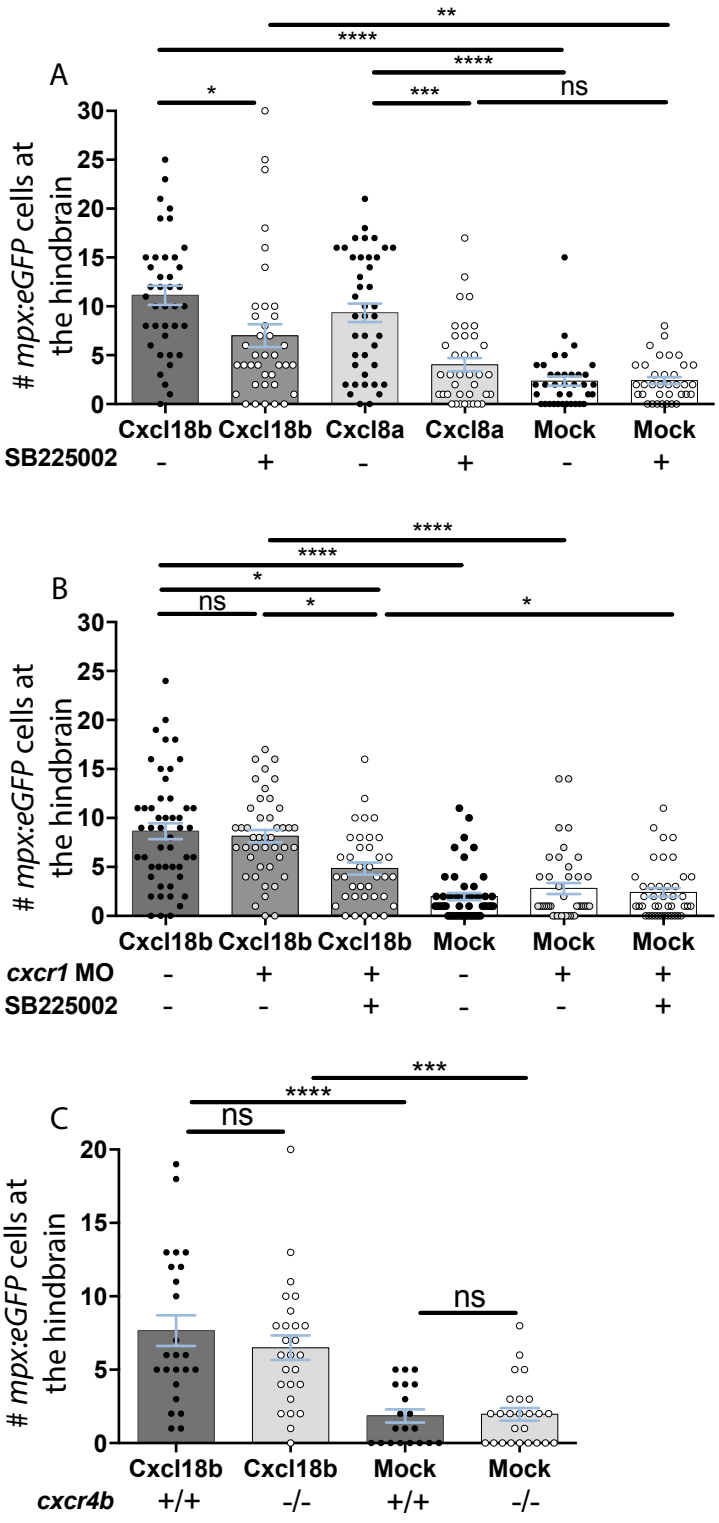
A
mpx:eGFP cells at the hindbrain
Cxcl18b Cxcl18b Cxcl8a Cxcl8a Mock Mock
SB225002 - + - + - +
B
mpx:eGFP cells at the hindbrain
Cxcl18b Cxcl18b Cxcl18b Mock Mock Mock
cxcr1 MO - + + - + +
SB225002 - - + - - +
C
mpx:eGFP cells at the hindbrain
Cxcl18b Cxcl18b Mock Mock
cxcr4b +/+ -/- +/+ -/-
ns

Figure 2

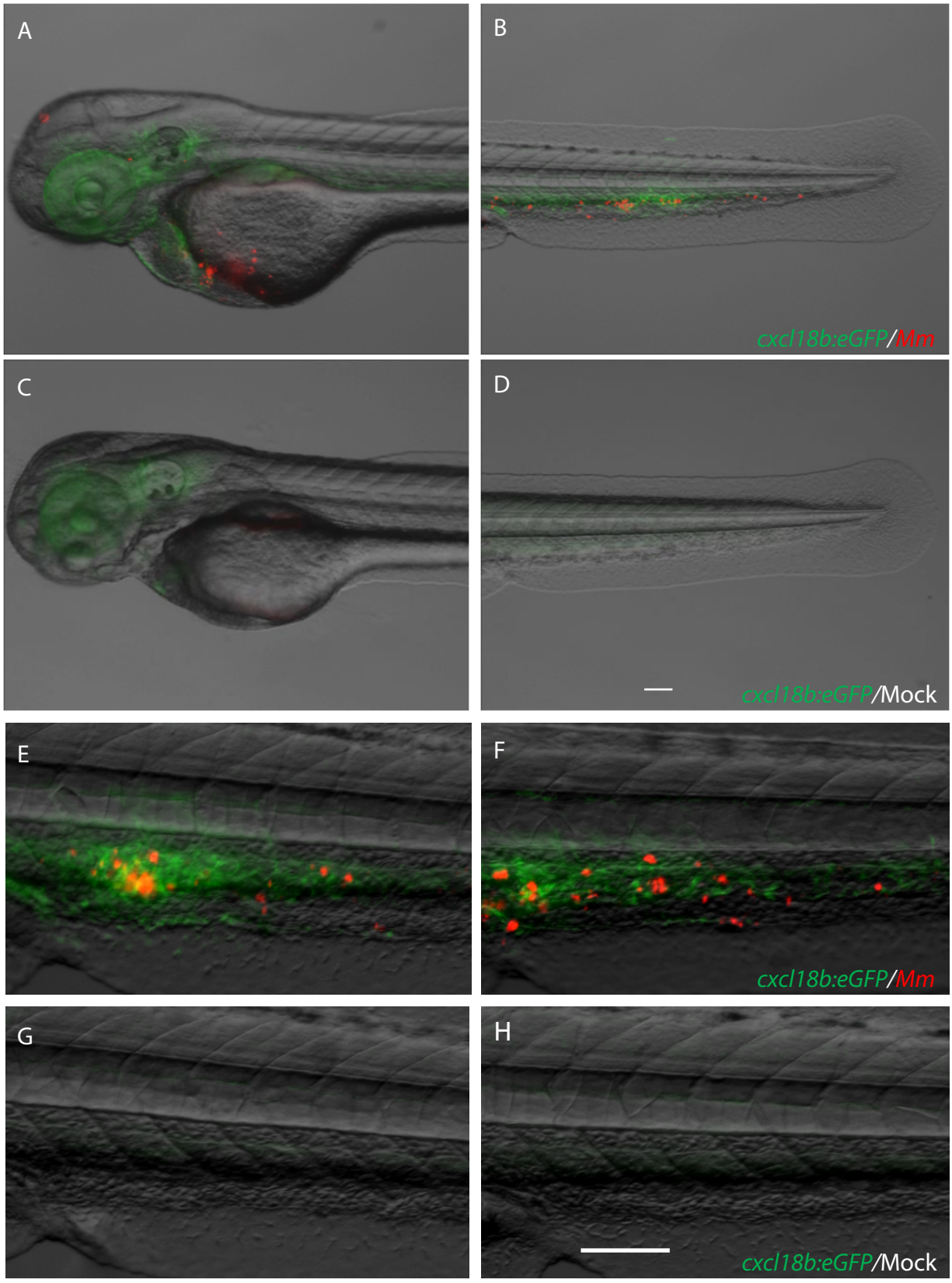
A
B
cxcl18b:eGFP/Mm
C
D
cxcl18b:eGFP/Mock
E
F
cxcl18b:eGFP/Mm
G
H
cxcl18b:eGFP/Mock

Figure 3

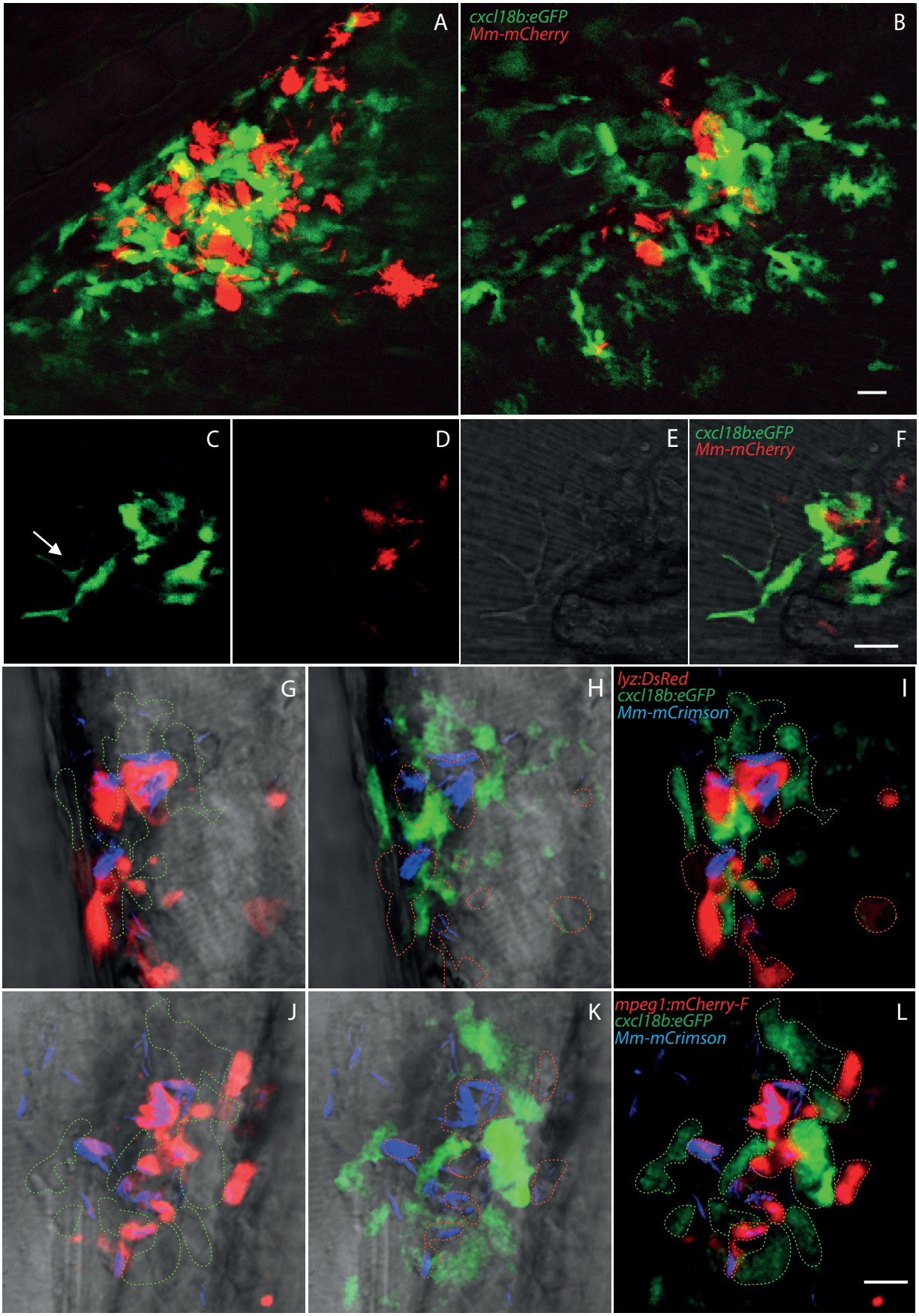
A
cxcl18b:eGFP
Mm-mCherry
B
C
D
E
cxcl18b:eGFP
Mm-mCherry
F
G
H
lyz:DsRed
cxcl18b:eGFP
Mm-mCrimson
I
J
K
mpeg1:mCherry-F
cxcl18b:eGFP
Mm-mCrimson
L

Figure 4

A

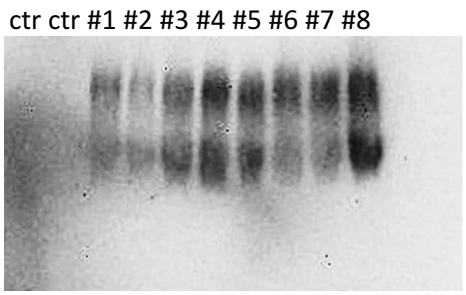

L

B

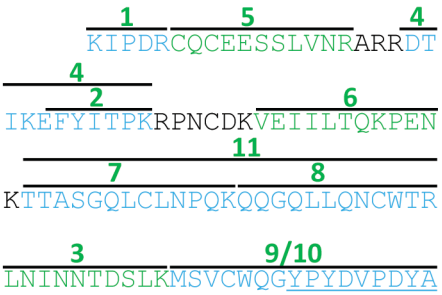

C

CXCLc1c_HA Mass: 11828 Score: 1704 Queries matched: 90 emPAI: 11.70

Query	Observed	Mr(expt)	Mr(calc)	ppm	Miss	Score	Expect	Rank	Peptide	
17	314.6928	627.3710	627.3704	0.90	1	30	0.019	1	-.KIPDR.C	1
244	449.2398	896.4650	896.4644	0.75	0	43	0.0012	1	K.EFYITPK.R	2
565	566.3031	1130.5916	1130.5931	-1.36	0	35	0.015	1	R.LNINNTDSLK.M	3
1118	677.8694	1353.7242	1353.7180	4.55	1	64	1.3e-05	1	R.DTIKEFYITPK.R	4
1222	691.2958	1380.5771	1380.5762	0.66	0	69	1e-06	1	R.CQCEESSLVNR.A	5
1333	706.4123	1410.8101	1410.8082	1.36	0	74	8.5e-07	1	K.VEIILTQKPENK.T	6
1353	709.3580	1416.7014	1416.7031	-1.23	0	87	8.3e-08	1	K.TTASGQLCLNPQK.Q	7
1784	766.3750	1530.7355	1530.7361	-0.43	0	66	9.5e-06	1	K.QQGQLLQNCWTR.L	8
2938	975.9084	1949.8022	1949.7964	2.95	0	38	0.00064	1	K.MSVCWQGYPYDVPDYA.-	9
2988	983.9038	1965.7930	1965.7914	0.84	0	(30)	0.0039	1	K.MSVCWQGYPYDVPDYA.-	10
4249	977.4811	2929.4215	2929.4287	-2.47	1	72	1.9e-06	1	K.TTASGQLCLNPQKQQGQLLQNCWTR.L	11

Supplementary Figure S1